ACS APPLIED MATERIALS & INTERFACES

Research Article

www.acsami.org

Significant Enhancement in the Thermoelectric Performance of a Bismuth Telluride Nanocompound through Brief Fabrication Procedures

Cham Kim,*[,†,‡] Dong Hwan Kim,[†] Hoyoung Kim,[†] and Jong Shik Chung*[,‡]

[†]Daegu Gyeongbuk Institute of Science and Technology (DGIST), 50-1 Sang-ri, Hyeonpung-myeon, Dalseong-gun, Daegu 711-873, Republic of Korea

[‡]Department of Chemical Engineering, Pohang University of Science and Technology (POSTECH), San 31 Hyoja-dong, Pohang 790-784, Republic of Korea

Supporting Information

ABSTRACT: A binary BiTe nanocompound for thermoelectric applications was prepared via a water-based chemical reaction under atmospheric conditions. We attempted to increase the carrier mobility of the nanocompound by adopting a post-thermal treatment consisting of calcination and reduction at different temperatures. We also tried to control the carrier density of the compound by adjusting the stoichiometry of the atomic constituents. We measured other transport properties (i.e., electrical resistivity, Seebeck coefficient, and thermal conductivity) and observed how these properties were affected by both the carrier mobility and the carrier density. We derived the thermoelectric performance, as captured by the figure of merit (ZT), from the transport properties and discussed the effect of such properties on the ZT value. The nanocompound exhibited a very competent ZT value (0.91 at 100 °C), which is one of the best thermoelectric performances of chemically synthesized BiTe materials.

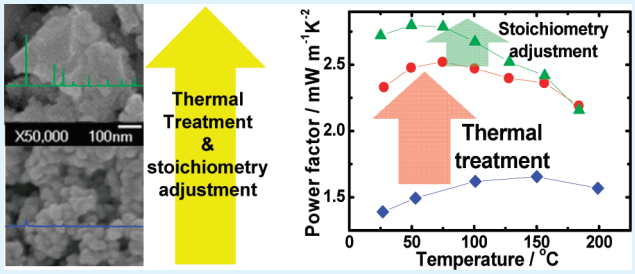

KEYWORDS: *thermoelectric materials, ZT, chemical synthesis, nanostructures, bismuth telluride*

1. INTRODUCTION

Thermoelectric (TE) technology has been intensively investigated due to its attractive applications, such as waste heat-to-electricity conversion and solid-state cooling.[1−7] In this field, one of the main topics has always been how to improve the performance of TE materials to increase the efficiency of energy conversion. The comprehensive performance of such materials is evaluated via the dimensionless figure of merit ZT (= $\alpha^2\sigma T/\kappa$), in which α is the Seebeck coefficient, σ is the electrical conductivity, T is the absolute temperature, and κ is the thermal conductivity.[5−10] Therefore, an excellent TE material should have high σ and low κ, characteristics indicative of a so-called phonon-glass/electron-crystal (PGEC).[1,7−15]

With the meteoric development in nanotechnology, many groups have been trying to build low-dimensional structures to serve as a type of PGEC material. Reports have shown that ZT can be enhanced in the structures of quantum dots (QD) and superlattice (SL) thin films due to the increase in the power factor ($\alpha^2\sigma$) and the decrease in κ, which result from quantum confinement and the phonon scattering effect, respectively.[13−21] Relatively high ZT values were often exhibited in these QDs or SL structures, but the commercialization of these substances is generally difficult due to complicated production processes and high cost. Therefore, some groups have focused on an approach that compacts these materials into nanobulk structures composed of nanoparticles,[22−24] nanotubes,[25−27] and nanowires.[28−30] Not only do these nanostructures still exhibit the phonon scattering effect, which reduces κ, but they can also be prepared with relatively inexpensive methods.

Many researchers have tried to fabricate BiTe nanomaterials via a wet chemical synthesis process because one can easily obtain the nanomaterials having various morphologies with the bottom-up process. This process mostly resulted in poor ZT values; nevertheless, all of the nanomaterials showed remarkable reductions in thermal conductivity.[31−35] A variety of chemical additives are used to realize diverse nanostructures in a chemical synthesis process but it is not considered that the additives are completely removed by a washing step. In addition, the stoichiometry of a final product could possibly be different from desired stoichiometry because precursors are used as raw materials. For these reasons, chemically synthesized BiTe nanocompounds might show poor electrical properties (i.e., carrier mobility, electrical conductivity, and Seebeck coefficient), resulting in low ZT values; however, most researchers have only emphasized low thermal conductivities obtained from their nanomaterials. It was barely done to

Received: February 17, 2012
Accepted: May 15, 2012
Published: May 15, 2012

   dx.doi.org/10.1021/am3002764 | ACS Appl. Mater. Interfaces 2012, 4, 2949−2954

investigate the procedures focused on improving the poor electrical properties; thus, we have intensively studied how to improve the electrical properties of our nanomaterials for high ZT value.

In a previous study, we fabricated BiTe nanocompounds composed of aggregated nanoparticles via inexpensive and brief chemical synthesis routes, and the compounds were sintered to achieve a small degree of grain growth.[36,37] We reported that the thermoelectric performance of the nanocompounds was not satisfactory compared with that of single-crystal BiTe because of their low Seebeck coefficient − high carrier density seemed to cause the low Seebeck coefficient. The negative aspects of having a low Seebeck coefficient in the nanocompounds overwhelmed the benefit of the low thermal conductivity. To improve the nanocompounds, we investigated the influence of the stoichiometric ratio of the bismuth constituent on a Seebeck coefficient and an electrical resistivity[38] and reported that the increased Seebeck coefficient was accompanied by increased electrical resistivity. Organic chemical additives were employed to obtain a reactive bismuth source in the chemical synthesis process; however, these additives might not be completely removed during the washing step. We assumed that these organic residues attenuated the effective charge carrier mobility, resulting in a significant increase in the electrical resistivity. Therefore, we focused on the thermal treatment of the as-synthesized BiTe powder to eliminate the residual organic chemicals and to increase the crystallinity of the powder. In addition, we decreased the tellurium ratio by adjusting the stoichiometry of the atomic constituents to decrease the carrier density because more organic chemical additives must be used to increase the stoichiometric ratio of bismuth.

Research into a BiTe-based nanocompound has mostly been performed on the p-type semiconductor, $Bi_xSb_{2-x}Te_3$, because it basically exhibits a high power factor.[12,14,38] The $Bi_xSb_{2-x}Te_3$ nanocompound can even exhibit a low thermal conductivity, and thus the p-type nanocompound has an excellent ZT value, up to 1.4.[24] Both p-type and n-type materials are required to constitute thermoelectric modules, but an n-type BiTe nanocompounds still show relatively low ZT values, likely because of their low power factors.[38] This is why researchers should develop an n-type BiTe nanocompound having a high thermoelectric performance. In this work, we successfully increased a power factor of our n-type nanocompound by adopting the series of brief and reproducible supplementary procedures, which were explained above. We achieved a ZT value in the vicinity of 1.0 due to the synergetic effect of the increased power factor and the basically low thermal conductivity of our nanocompound. The obtained ZT is one of the highest thermoelectric performances for n-type BiTe binary materials.

2. EXPERIMENTAL SECTION

2.1. Chemicals. Bismuth(III) nitrate ($Bi(NO_3)_3$, Kojundo Chemical, 99.99%) and elemental tellurium powder (Te, Kojundo Chemical, 99.999%, 45 μm) were employed as precursors. Ascorbic acid ($C_6H_8O_6$, Junsei Chemicals, 99%) and ethylenediaminetetraacetic acid (EDTA: $C_{10}H_{16}N_2O_8$, Junsei Chemicals, 99.4%) were used to dissolve the bismuth precursor and to stabilize the bismuth ion obtained from the precursor in deionized water, respectively. Sodium borohydride ($NaBH_4$, Samchun, 99%) was used to reduce the Te powder. All of the chemicals were used without further purification.

2.2. Sample Preparation. On the basis of the procedure reported in our previous work,[37] a binary thermoelectric material, BiTe, was fabricated and a reaction mechanism was suggested (Schemes S1−S3 in the Supporting Information). Sixty millimoles of $Bi(NO_3)_3$ was mixed with deionized water, and the chemicals such as ascorbic acid and EDTA were added. The resulting pale yellow suspension was vigorously stirred until it reached a stable pH value (ca. pH 1.5). Then, an NaOH solution (5.0 M) was slowly injected into the mixture to adjust the pH to 11, at which point a yellow cloudy solution was obtained without any undissolved particles. This solution became completely transparent after additional stirring for ca. 3 h (solution A). Meanwhile, various amounts of Te were individually placed in three-neck round-bottom flasks filled with an NaOH solution, after which the reducing agent, $NaBH_4$(aq), was added. These Te mixtures were heated to 90 °C with vigorous stirring. When the mixtures completely turned into transparent purple-colored solutions (reduced Te solutions), we poured solution A into each Te solution at once. Black precipitates instantly appeared; they were then aged for 60 h. Next, each precipitate was filtered and rinsed thoroughly using dry ethanol and deionized water. After the precipitates were dried under vacuum at 60 °C overnight, black powders were finally obtained. We preferentially calcined the powders at 250 °C for 6 h, and then treated them at various temperatures under H_2 atmosphere for 6 h (reduction). After the series of thermal treatments, the powders were individually sintered with a spark plasma sintering machine (SPS; DR. Sinter, SPS-3, 20MK-IV) at 400 °C under a pressure of 50 MPa in an Ar atmosphere. The heating rate was 80 K min^{-1}, and the holding time at the sintering temperature was 10 min.

2.3. Characterization Studies. Powder X-ray diffraction (XRD) patterns were collected with a D/MAX-2500 diffractometer (Rigaku) using Cu Kα radiation and a scintillation counter detector. Relevant patterns were recorded over a 2θ range of 15−70°. Field emission scanning electron micrographs (FE-SEM) were obtained using an S-4800 microscope (Hitachi) to observe the relevant morphology. Electron backscattering diffraction (EBSD) analysis was conducted with a Hitachi S-4300SE scanning electron microscope. Evaluation for a chemical composition was performed with an electron probe microanalyzer (EPMA, JXA 8900R, JEOL) equipped with a wavelength dispersive X-ray spectrometer (WDS). The electrical resistivity (ρ) and Seebeck coefficient (α) were measured simultaneously with an LSR-3 instrument (Linseis Thermal Analysis). Carrier mobility was calculated with the equation: $\mu = 1/(\rho ne)$, where e is electric charge, 1.6×10^{-19} C. Carrier density (n) was measured by using an HL5500PC-M (Bio-Rad) Hall-effect measurement system. The thermal conductivity (κ) is related to the thermal diffusivity (λ) through the equation: $\kappa = \lambda C_p d$, where d and C_p denote the density and specific heat capacity of the sample, respectively. The thermal diffusivities of the samples between 300 and 573 K were measured with a laser flash tool (LFA447, Netzsch). The density was approximately 98% of the theoretical density for a Bi_2Te_3 bulk material, 7.878 g cm^{-3}.[14] We measured the specific heat capacity by using a differential scanning calorimeter (DSC200, Netzsch) and presented it with the calculated C_p value based on a literature[39] (Figure S1 in Supporting Information). We adopted the measured values of λ and C_p to calculate the thermal conductivity using the above equation. The thermal conductivity is roughly determined by the sum of the carrier thermal conductivity (κ_e) and the lattice thermal conductivity (κ_L). Because the carrier thermal conductivity can be calculated by the Wiedemann−Franz law, $\kappa_e = L_0\sigma T$, where L_0 and σ are the Lorenz number and the electrical conductivity, respectively, the lattice thermal conductivity can also be estimated. Consequently, the figures of merit of all samples were calculated with the following equation: $ZT = \alpha^2\sigma T/\kappa$.

3. RESULTS AND DISCUSSION

Figure 1 shows the XRD patterns of the BiTe powders following the thermal treatment. The calcination temperature of 250 °C (denoted as C250) was chosen by considering the thermal degradation temperature of the organic chemical additive EDTA, which is the most thermally resistive of the additives used.[40] The calcined sample showed new diffraction

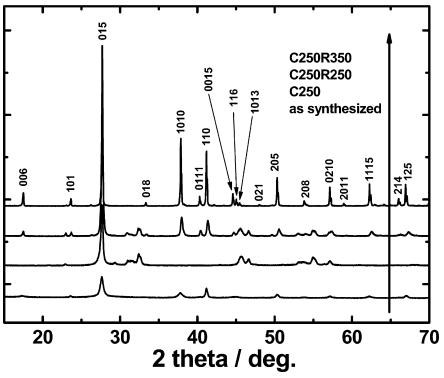

Figure 1. XRD patterns of the BiTe powder after various thermal treatments.

peaks in certain 2θ ranges (30−35°, 45−50°, and 55−60°) that were not observed in the as-synthesized nanocompound, indicating the presence of oxidized species.[36,37] We tried to reduce the calcined sample by heating it again under an H_2 atmosphere (denoted as R). When we reheated the calcined sample to 250 °C (C250R250), we still detected oxidized species in those 2θ ranges. The oxidized species finally disappeared when we heated the calcined sample to 350 °C under an H_2 atmosphere (C250R350), and a diffraction pattern similar to that of the as-synthesized nanocompound appeared. The diffraction pattern of C250R350 consisted of many diffraction lines of various planes, which coincide with the diffraction lines of the rhombohedral Bi_2Te_3 (JCPDS card No. 85−0439, 82−0358). It is unclear whether the residues and the oxidized species were completely eliminated by the thermal treatment; thus, we are currently conducting an elemental (C, H, O, and N) analysis. We plan to adjust the conditions (temperature and time) of the thermal treatment when the results are derived from the analysis.

We postulated that particle growth must have occurred because the crystallinity significantly increased after the thermal treatment. According to the SEM images (Figure 2), the

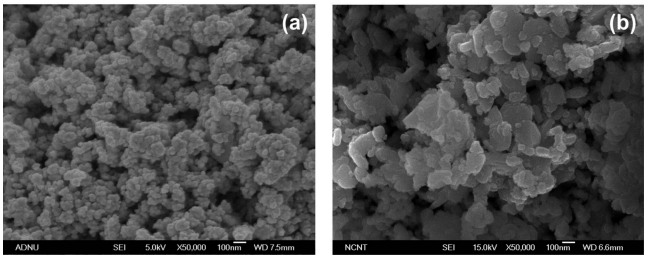

Figure 2. Morphology of the BiTe nanocompound according to the thermal treatment: (a) as-synthesized and (b) heat-treated.

particle growth could be clearly observed after the treatment; however, the growth did not seriously impair the existing rate of phonon scattering considering the long mean free path of a phonon (0.1−10 μm)[37,38,41] and the grain size difference in sintered specimens caused by the thermal treatment (see Figure S2 in the Supporting Information). We measured the total thermal conductivity before and after the thermal treatment and calculated the lattice (κ_L) and carrier (κ_e) thermal conductivities, respectively. As presented in Figure 3a, we confirmed that the total thermal conductivity increased somewhat after the thermal treatment. Both terms (κ_L, κ_e) of the thermal conductivity increased, but the rate of increase was considerably smaller in the lattice term, which is closely related to phonon scattering, than in the carrier term, especially below 100 °C. We thought that the increase in carrier thermal conductivity was the main cause of the total thermal conductivity increase below 100 °C. In addition, we observed that the electrical resistivity decreased while the Seebeck coefficient increased after the thermal treatment (Figure 3b, c). It is an encouraging phenomenon in thermoelectrics that the electrical conductivity and the Seebeck coefficient increase simultaneously. We were able to greatly improve the power factor of the nanocompound (above 60% at 25 °C) through the thermal treatment (Figure 3d).

We measured the carrier mobility and carrier density before and after the thermal treatment at 25 °C, and the data are presented in Table 1 along with other properties measured at the same temperature. The carrier mobility was improved greatly after the treatment because the chemical residues were removed from the nanocompound; in addition, the crystallinity of the nanocompound greatly increased. We thought that the carrier thermal conductivity increased considerably after the treatment because of the improved carrier mobility. The carrier density seemed to decrease after the treatment because tellurium is known to evaporate more easily than bismuth during various thermal processes. Despite the decrease in the carrier density after the treatment, the resistivity decreased because of the improvement in carrier mobility. The Seebeck coefficient increased due to the decrease in the carrier density, but it might be still low for thermoelectric applications − the Seebeck coefficient is quite lower than that of other Bi_2Te_3.[42,43] Because a BiTe-type thermoelectric material is known to show optimized thermoelectric properties when a carrier density ranges from 1×10^{18} to 1×10^{19} cm^{-3},[44,45] we expect that the carrier density after the thermal treatment (6.53×10^{19} cm^{-3}, Table 1) should be even lower.

Because we employed a metal precursor (i.e., $Bi(NO_3)_3$) for synthesizing the nanocompound, the actual amount of metal in the precursor could be different from the theoretical amount of metal according to the precursor stoichiometry.[38] In other words, we might obtain a final product with a somewhat different stoichiometric ratio compared to the intended ratio. We assumed that the amount of bismuth in $Bi(NO_3)_3$ was less than we can infer from its stoichiometry; thus, we obtained a tellurium-rich compound with a high carrier density, as presented in Table 1. We tried to use a lower amount of tellurium in the synthesis process to decrease the carrier density. Because the molar ratio of tellurium was initially fixed at 3.0, we decreased it to 2.5 and 2.0, respectively. It was confirmed that the tellurium ratio in a final bulk specimen was gradually reduced as smaller amount of tellurium was used in the synthesis step (see Figure S3 in Supporting Information). According to the XRD patterns shown in Figure 4, each sample maintained the rhombohedral phase of bismuth telluride with no other peaks indicating secondary phases.

All transport properties varied depending on the adjusted tellurium stoichiometry (Table 2, Figure 5). When we sequentially reduced the molar ratio of tellurium from 3.0 to 2.0, the carrier density gradually decreased, as shown in Table 2. Both the electrical resistivity and the Seebeck coefficient gradually increased with the decrease in the carrier density. As the tellurium stoichiometry was reduced, the electrical resistivity uniformly increased at most of the measured temperatures (Figure 5a), whereas the Seebeck coefficient

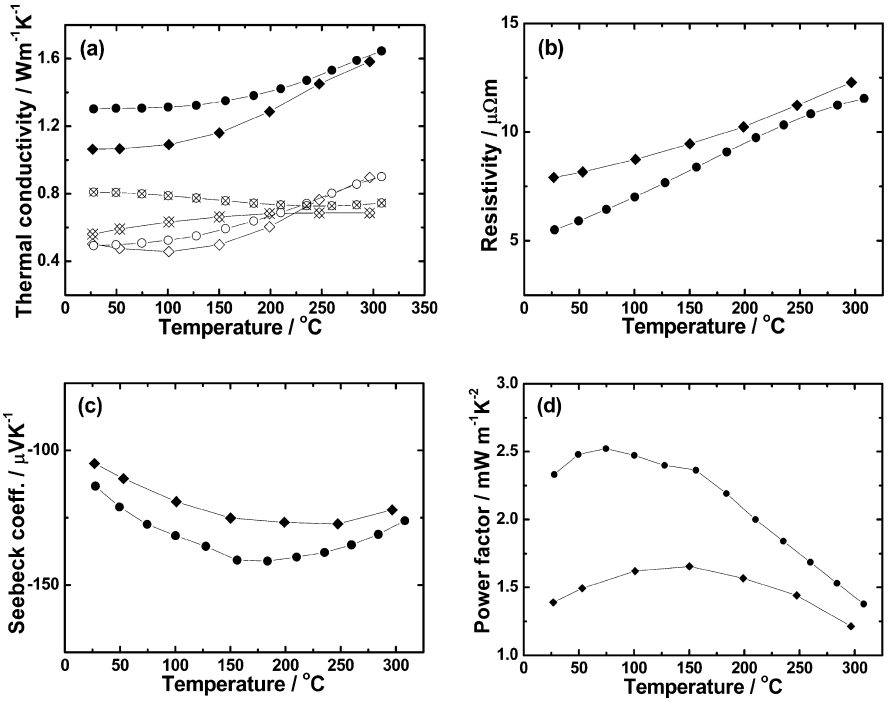

Figure 3. Thermoelectric transport properties of the BiTe nanocompound according to the thermal treatment (♦, as-synthesized; ●, heat-treated): (a) total thermal conductivity with lattice (κ_L—◇, ○) and carrier (κ_e—diamond with x, circle with x) terms, (b) electrical resistivity, (c) Seebeck coefficient, and (d) power factor.

Table 1. Thermoelectric Transport Properties of the BiTe Nanocompound at 25 °C with and without the Thermal Treatment

thermal treatment	carrier mobility ($cm^2\ V^{-1}\ s^{-1}$)	carrier density ($\times 10^{19}\ cm^{-3}$)	carrier thermal conductivity ($W\ m^{-1}\ K^{-1}$)	resistivity ($\mu\Omega$ m)	Seebeck coefficient ($\mu V\ K^{-1}$)
no	117	6.75	0.56	7.9	−105
yes	174	6.53	0.81	5.5	−113

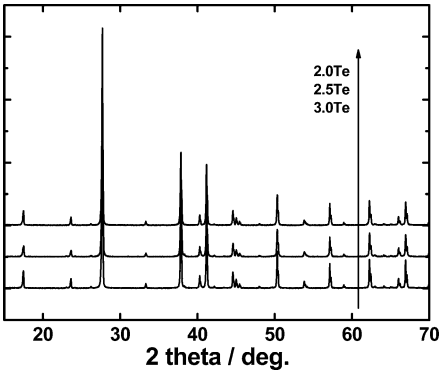

Figure 4. XRD patterns of heat-treated BiTe containing different molar ratios of tellurium.

Table 2. Thermoelectric Transport Properties of the Heat-Treated Bite Nanocompound with Different Stoichiometric Ratios of Tellurium at 25 °C

molar ratio of Te	carrier density ($\times 10^{19}\ cm^{-3}$)	resistivity ($\mu\Omega$ m)	Seebeck coefficient ($\mu V\ K^{-1}$)	carrier thermal conductivity ($W\ m^{-1}\ K^{-1}$)
3.0	6.53	5.5	−113	0.81
2.5	5.79	6.3	−127	-
2.0	5.11	7.5	−143	0.59

irregularly increased. Specifically, the increase rates of the Seebeck coefficient were biased toward the low-temperature region (below 150 °C), as shown in Figure 5b. Considering that BiTe-type compounds are thermoelectric materials suitable for low-temperature operations, the atomic composition of our nanocompound seems to be close to the ideal stoichiometry. Despite the increase in the electrical resistivity, the power factor was improved by ca. 18% at room temperature because of the greater increment in the Seebeck coefficient (Figure 5c). We also confirmed that the increase rate of the power factor was intensified in the low-temperature region because of the Seebeck coefficient. The carrier thermal conductivity decreased due to the decrease in the carrier density. When the lowest molar ratio was adopted, we obtained a value at 25 °C (0.59 W $m^{-1}\ K^{-1}$, Table 2) similar to what the nanocompound exhibited before the thermal treatment (0.56 W $m^{-1}\ K^{-1}$, Table 1). We assumed that the decrease in the carrier thermal conductivity was the main reason for the decrease in the total thermal conductivity because no remarkable change was found in the lattice term (Figure 5d). Namely, with the molar ratio of tellurium in 2.0, the lowest carrier density ($5.11 \times 10^{19}\ cm^{-3}$) was obtained and it led to the highest power factor and lower thermal conductivity (Figure 5c, d). As we mentioned above, thermoelectric properties of a BiTe-type material are usually optimized with a carrier density ranging from 1×10^{18} to $1 \times 10^{19}\ cm^{-3}$; thus, we have tried to reduce the carrier density by decreasing a tellurium composition even more. However, we obtained no further improvements in transport properties. We expect that the carrier density, $5.11 \times 10^{19}\ cm^{-3}$, should be an optimized value for a thermoelectric performance.

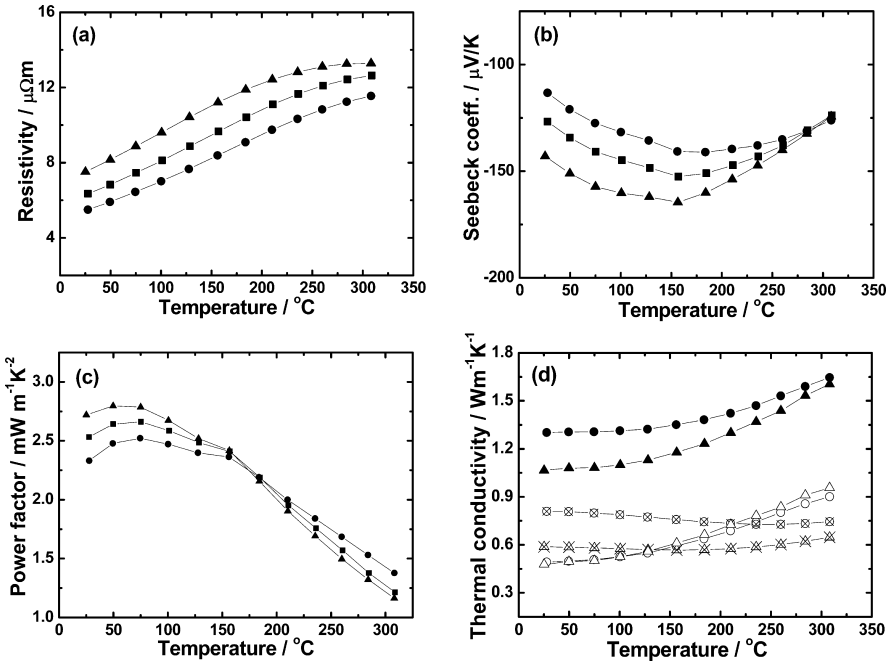

Figure 5. Thermoelectric transport properties of heat-treated BiTe containing different molar ratios of tellurium (3.0 (●, ○, circle with x), 2.5 (■), 2.0 (▲, △, triangle with x)): (a) electrical resistivity, (b) Seebeck coefficient, (c) power factor, and (d) total thermal conductivity divided into the lattice (κ_L—○,△) and carrier (κ_e—circle with x, triangle with x) terms.

We calculated the ZT values using the transport properties measured above (Figure 6). After the thermal treatment, the

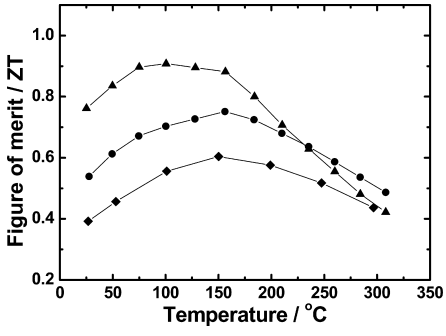

Figure 6. Figure of merit of BiTe nanocompounds with different molar ratios of Te: 3.0 (♦, as-synthesized; ●, heat-treated) and 2.0 (▲).

ZT values increased almost uniformly throughout the range of measured temperatures; the maximum ZT values appeared at nearly the same temperature. In contrast, the ZT values increased greatly, especially in the low-temperature region (below 150 °C), when we reduced the molar ratio of tellurium. The series of ZT improvements are closely related to the increase in carrier mobility after the thermal treatment and to the decrease in carrier density due to the stoichiometric adjustment. We greatly enhanced the ZT values of the compound compared with those of the compound without the thermal treatment and the stoichiometric adjustment (by 94% at 25 °C and 63% at 100 °C), which was reported in the previous work.[37] Namely, we achieved rather acceptable ZT values (i.e., 0.76 at 25 °C, a maximum of 0.91 at 100 °C) in the binary thermoelectric compound, BiTe.

4. CONCLUSION

We fabricated the BiTe nanocompound via a wet chemical reaction for thermoelectric applications. We tried to purify the nanocompound and to increase its crystallinity by employing a post-thermal treatment. This treatment resulted in greatly enhanced carrier mobility, which in turn reduced the electrical resistivity. We confirmed that the carrier density of the nanocompound was somewhat high for thermoelectric applications. We attempted to reduce the carrier density by decreasing the stoichiometric ratio of tellurium so that we could increase the Seebeck coefficient of the nanocompound significantly. After treating the as-synthesized nanocompound following the procedures outlined in this work, we were able to significantly improve the ZT value of the nanocompound.

■ ASSOCIATED CONTENT

Ⓢ Supporting Information

We gave chemical reaction mechanisms for the BiTe nanocompound with its specific heat capacity, inverse pole figure images, and average atomic ratios. This material is available free of charge via the Internet at http://pubs.acs.org.

■ AUTHOR INFORMATION

Corresponding Author

*Tel.: +82-54-279-2267 (J.S.C.); +82-53-785-3602 (C.K.). Fax: +82-54-279-8453 (J.S.C.); +82-53-785-3609 (C.K.). E-mail: jsc@postech.ac.kr (J.S.C.); charming0207@dgist.ac.kr (C.K.).

Notes

The authors declare no competing financial interest.

■ ACKNOWLEDGMENTS

This work was financially supported by the DGIST R & D Program of the Ministry of Education, Science and Technology (MoEST) of Korea (12-EN-01).

REFERENCES

(1) Dresselhaus, M. S.; Chen, G.; Tang, M. Y.; Yang, R. G.; Lee, H.; Wang, D. Z.; Ren, Z. F.; Fleurial, J. P.; Gogna, P. *Adv. Mater.* **2007**, *19*, 1043−1053.

(2) Dresselhaus, M. S.; Chen, G.; Tang, M. Y.; Yang, R. G.; Lee, H.; Wang, D. Z.; Ren, Z. F.; Fleurial, J. P.; Gogna, P. *Mater. Res. Soc. Symp. Proc.* **2005**, *886*, 0886−F01−01.

(3) Byrnes, D. F.; Heshmatpour, B. *Mater. Res. Soc. Symp. Proc.* **2005**, *886*, 0886−F12−03.

(4) Tritt, T. M.; Zhang, B.; Gothard, N.; He, J.; Ji, X.; Thompson, D.; Kolis, J. W. *Mater. Res. Soc. Symp. Proc.* **2005**, *886*, 0886−F02−01.

(5) Sootsman, J.; Kong, H.; Uher, C.; Downey, A.; D'Angelo, J. J.; Wu, C.-I.; Hogan, T.; Caillat, T.; Kanatzidis, M. *Mater. Res. Soc. Symp. Proc.* **2007**, *1044*, 1044−U08−01.

(6) Hsu, K. F.; Loo, S.; Guo, F.; Chen, W.; Dyck, J. S.; Uher, C.; Hogan, T.; Polychroniadis, E. K.; Kanatzidis, M. G. *Science* **2004**, *303*, 818−821.

(7) Ji, X.; Zhang, B.; Tritt, T. M.; Kolis, J. W.; Kumbhar, A. *J. Electron. Mater.* **2007**, *36*, 721−726.

(8) Zhu, T. J.; Liu, Y. Q.; Zhao, X. B. *Mater. Res. Bull.* **2008**, *43*, 2850−2854.

(9) Li, H.; Cai, K. F.; Wang, H. F.; Wang, L.; Li, X. L. *Key Eng. Mater.* **2008**, *368*−*372*, 550−552.

(10) Martin, J.; Nolas, G. S.; Zhang, W.; Chen, L. *Appl. Phys. Lett.* **2007**, *90*, 222112.

(11) Snyder, G. J.; Christensen, M.; Nishibori, E.; Caillat, T.; Iversen, B. B. *Nat. Mater.* **2004**, *3*, 458−463.

(12) Nolas, G. S.; Sharp, J.; Goldsmid, H. J. *Thermoelectrics: Basic Principles and New Materials Developments*; Springer: Berlin, 2001.

(13) Kurosaki, K.; Matsuda, T.; Uno, M.; Kobayashi, S.; Yamanaka, S. *J. Alloys Compd.* **2001**, *319*, 271−275.

(14) Goldsmid, H. J. *Introduction to Thermoelectricity*; Springer: Berlin, 2009.

(15) Peng, J.; He, J.; Alboni, P. N.; Tritt, T. M. *J. Electron. Mater.* **2009**, *38*, 981−984.

(16) Nolas, G. S.; Morelli, D. T.; Tritt, T. M. *Annu. Rev. Mater. Sci.* **1999**, *29*, 89−116.

(17) Min, G.; Rowe, D. M. *J. Mater. Sci. Lett.* **1999**, *18*, 1305−1306.

(18) Grytsiv, A.; Rogl, P.; Berger, S.; Paul, C.; Michor, H.; Bauer, E.; Hilscher, G.; Godart, C.; Knoll, P.; Musso, M.; Lottermoser, W.; Saccone, A.; Ferro, R.; Roisnel, T.; Noel, H. . *Phys.: Condens. Matter* **2002**, *14*, 7071−7090.

(19) Tang, J.; Rachi, T.; Kumashiro, R.; Avila, M. A.; Suekuni, K.; Takabatake, T.; Guo, F. Z.; Kobayashi, K.; Akai, K.; Tanigaki, K. *Phys. Rev. B* **2008**, *78*, 085203.

(20) Hermann, R. P.; Grandjean, F.; Keppens, V.; Schweika, W.; Nolas, G. S.; Mandrus, D. G.; Sales, B. C.; Christen, H. M.; Bonville, P.; Long, G. J. *Mater. Res. Soc. Symp. Proc.* **2005**, *886*, 0886−F10−01.

(21) Paschen, S.; Pacheco, V.; Bentien, A.; Sanchez, A.; Carrillo-Cabrera, W.; Baenitz, M.; Iversen, B. B.; Grin, Y.; Steglich, F. *Physica B* **2003**, *328*, 39−43.

(22) Deng, Y.; Zhou, X.; Wei, G.; Liu, J.; Nan, C. W.; Zhao, S. *J. Phys. Chem. Solids* **2002**, *63*, 2119−2121.

(23) Ji, X.; Zhao, X.; Zhang, Y.; Lu, B.; Ni, H. *Mater. Res. Soc. Symp. Proc.* **2004**, 793−S1.4.

(24) Poudel, B.; Hao, Q.; Ma, Y.; Lan, Y.; Minnich, A.; Yu, B.; Yan, X.; Wang, D.; Muto, A.; Vashaee, D.; Chen, X.; Liu, J.; Dresselhaus, M. S.; Chen, G.; Ren, Z. *Science* **2008**, *320*, 634−638.

(25) Zhao, X. B.; Ji, X. H.; Zhang, Y. H.; Zhu, T. J.; Tu, J. P.; Zhang, X. B. *Appl. Phys. Lett.* **2005**, *86*, 062111.

(26) Hone, J.; Ellwood, I.; Muno, M.; Mizel, A.; Cohen, M. L.; Zettl, A.; Rinzler, A. G.; Smalley, R. E. *Phys. Rev. Lett.* **1998**, *80*, 1042−1045.

(27) Cao, Y. Q.; Zhu, T. J.; Zhao, X. B. *J. Alloys Compd.* **2008**, *449*, 109−112.

(28) Lu, J.; Han, Q.; Yang, X.; Lu, L.; Wang, X. *Mater. Lett.* **2007**, *61*, 3425−3428.

(29) Zhao, X. B.; Ji, X. H.; Zhang, Y. H.; Lu, B. H. *J. Alloys Compd.* **2004**, *368*, 349−352.

(30) Sun, T.; Zhao, X. B.; Zhu, T. J.; Tu, J. P. *Mater. Lett.* **2006**, *60*, 2534−2537.

(31) Zhang, Y.; Wang, H.; Kräemer, S.; Shi, Y.; Zhang, F.; Snedaker, M.; Ding, K.; Moskovits, M.; Snyder, G. J.; Stucky, G. D. *ACS Nano* **2011**, *5*, 3158−3165.

(32) Sun, Z.; Liufu, S.; Yao, Q.; Chen, L. *Mater. Chem. Phys.* **2010**, *121*, 138−141.

(33) Scheele, M.; Oeschler, N.; Meier, K.; Kornowski, A.; Klinke, C.; Weller, H. *Adv. Funct. Mater.* **2009**, *19*, 3476−3483.

(34) Li, S.; Zhang, S.; He, Z.; Toprak, M.; Stiewe, C.; Muhammed, M.; Müller, E. *J. Nanosci. Nanotechnol.* **2010**, *10*, 7658−7662.

(35) Purkayastha, A.; Jain, A.; Hapenciuc, C.; Buckley, R.; Singh, B.; Karthik, C.; Mehta, R. J.; Tasciuc, T. B.; Ramanath, G. *Chem. Mater.* **2011**, *23*, 3029−3031.

(36) Kim, C.; Kim, D. H.; Han, Y. S.; Chung, J. S.; Park, S. H.; Park, S.; Kim, H. *Mater. Res. Bull.* **2011**, *46*, 407−412.

(37) Kim, C.; Kim, D. H.; Han, Y. S.; Chung, J. S.; Park, S. H.; Kim, H. *Powder Tech.* **2011**, *214*, 463−468.

(38) Kim, C.; Kim, D. H.; Kim, J. S.; Han, Y. S.; Chung, J. S.; Kim, H. *J. Alloys Compd.* **2011**, *509*, 9472−9478.

(39) Binnewies, M.; Milke, E. *Thermochemical Data of Elements and Compounds*; Wiley-VCH: Weinheim, Germany, 1999.

(40) Motekaitis, R. J.; Cox, X. B.; Taylor, P.; Martell, A. E.; Miles, B.; Tvedt, T. J. *Can. J. Chem.* **1982**, *60*, 1207−1213.

(41) Blakemore, J. S. *Solid State Physics*; Cambridge University Press: Cambridge, U.K., 1985.

(42) Fleurial, J. P.; Gailliard, L.; Triboulet, R.; Scherrer, H.; Scherrer, S. *J. Phys. Chem. Solids* **1988**, *49*, 1237−1247.

(43) Fu, J.; Song, S.; Zhang, X.; Cao, F.; Zhou, L.; Li, X.; Zhang, H. *Cryst. Eng. Comm.* **2012**, *14*, 2159−2165.

(44) Je, K. C.; Im, H. J.; Kim, D. H.; Kang, Y. J.; Ahn, J. S.; Kim, H. M.; Mitani, T. *Jpn. J. Appl. Phys.* **2003**, *42*, 3556−3559.

(45) Im, H. J.; Kim, D. H.; Mitani, T.; Je, K. C. *Jpn. J. Appl. Phys.* **2004**, *43*, 1094−1099.